

Pt-CeO_x/MWCNT electrocatalysts as ethanol-tolerant ORR cathodes for Direct Alcohol Fuel Cells

F.J. Rodriguez Varela,^{1,*} A.A. Gaona Coronado,² J.C. Loyola², Qi-Zhong Jiang³ and P. Bartolo Perez⁴

¹Nanosciences and Nanotechnology Program, CINVESTAV Unidad Saltillo, Carr. Saltillo-Monterrey Km. 13.5, Ramos Arizpe, Coahuila, C.P. 25900, México

²Instituto Tecnológico de Saltillo, V. Carranza 2400, Col. Tecnológico, C.P. 25280, Saltillo, Coahuila México.

³Department of Chemical Engineering, Shanghai Jiao Tong University, Shanghai, China, 200240

⁴CINVESTAV-IPN, Unidad Mérida, Departamento de Física Aplicada, A. P. 73 Cordemex, 97310, Mérida, Yuc., Mexico

Received: November 01, 2010, Accepted: February 01, 2011, Available online: April 06, 2011

Abstract: High performance 20% Pt-CeO_x (1:1 Pt:Ce weight ratio) electrocatalyst dispersed on Multiwalled Carbon Nanotubes (MWCNTs) was synthesized under H₂ atmosphere at 300 °C. The average particle size determined from XRD was ca. 1.7 and 10 nm for Ce and Pt, respectively. HRTEM analysis confirmed the presence of particle sizes within this range, although it was not possible to distinguish Ce from Pt nanoparticles. The XPS spectrum of Ce showed characteristics that indicate the existence of both oxidized and reduced phases (i.e., Ce₂O₃ and CeO₂). It is suggested that the presence of the Ce³⁺ state establishes the capacity of this material to act as a tolerant cathode. The spectrum of Pt confirmed the presence of Pt metal. The 20% Pt-CeO_x/MWCNT cathode showed high electroactivity for the Oxygen Reduction Reaction (ORR). Moreover, this novel material presented a high degree of tolerance to ethanol. During polarization tests in ethanol-containing solution, the Pt-CeO_x/MWCNT cathode showed no peak current density due to the ethanol oxidation reaction (EOR) and the onset potential for the ORR ($E_{\text{onset}}^{\text{ORR}}$) shifted by only 80 mV towards more negative potentials. Thus, the presence of ceria clearly enhanced the electrochemical tolerance of the Pt-based cathode to ethanol.

Keywords: Pt-CeO_x cathodes, ORR, tolerance to ethanol, Direct Alcohol Fuel Cells

1. INTRODUCTION

The development of highly selective and tolerant ORR cathodes, aimed at the reduction of efficiency losses in DAFCs due to the crossover effect, has received considerable attention in recent years [1-3]. Mainly bi- or tri-metallic electrocatalysts have been reported as suitable high performance cathodes for DAFCs [4-6], although some non-noble metals have shown important catalytic activity in the presence of organic molecules [7].

A recent approach in the development of tolerant-cathodes is related to the impregnation of Pt electrocatalysts with some materials having oxygen storage capacity [8-11]. In fact, the presence of such oxide materials that promote the formation of molecules that accelerate the kinetics of the ORR, also enhances the catalytic activity of Pt-based anodes for the oxidation of liquid fuels [12-

14]. A very attractive material with excellent capacity for oxygen reversible release, storage and transport is cerium oxide (CeO₂) [9, 10, 15]. The excellent properties of this oxide, which combined with Pt shows good behavior for the ORR in the presence of alcohols, have been reported elsewhere [9-10]. Particularly, the properties related to oxygen storage, including the shift between oxidized and reduced states (+3 and +4) are of interest. In fact, it might be this capability to switch valence states that determines the behavior of CeO₂ and the electroactivity of Pt-CeO₂ composite materials. This is relevant because in some recent reports, Pt-CeO₂ electrocatalysts are considered as highly active for the oxidation of ethanol or methanol [11-14, 16, 17]. The valence state of cerium oxide in such reports seems to be +4, thus forming an anode material with excellent properties for DAFCs. Meanwhile, the results in reference [10] clearly show the insensitivity of a cathode of composition Pt-CeO_x to the presence of methanol in oxygen saturated solution, i.e., a low catalytic activity as anode and high perform-

*To whom correspondence should be addressed:

Email: javier.varela@cinvestav.edu.mx

Phone: (52)-844-438-9612, Fax.: (52)-844-438-9610

ance as tolerant cathode. The report suggests that the valence state of cerium oxide in reference [10] might be +3 or between +3 and +4. Elsewhere, XPS analyses in reference [15] points out to an oxidized ceria phase of composition Ce_2O_3 that acts as co-catalyst in a high performance PtCo– CeO_x cathode. Therefore, by controlling the valence state of CeO_2 in Pt-based composite catalysts, it seems possible to design high performance anodes or cathodes for DAFCs.

In this work, we report the facile synthesis of a Pt- CeO_x /MWCNT cathode material with high activity for the ORR by thermal pyrolysis at relatively low temperatures under H_2 atmosphere. The electrocatalyst shows a high degree of selectivity towards the ORR in the presence of ethanol ($\text{C}_2\text{H}_5\text{OH}$). The cathode was characterized by XRD, EDS, HRTEM, XPS and electrochemical techniques.

2. EXPERIMENTAL

2.1. Synthesis of 20 % Pt- CeO_x /MWCNT

$\text{H}_2\text{PtCl}_6 \cdot 6\text{H}_2\text{O}$ (Alfa Aesar), $\text{Ce}(\text{NO}_3)_3 \cdot 6\text{H}_2\text{O}$ (Aldrich) and commercial MWCNT (MER Corp.) were used to synthesize the Pt- CeO_x /MWCNT cathode. The ratio between Pt and Ce was kept 1:1 in weight. The procedure was: MWCNTs were first functionalized by sonication in a HNO_3 :deionized water (DIW) solution (1:1 v/v) for 30 min, filtrated and washed with abundant DIW. Afterwards, 400 mg of MWCNT were ultrasonically dispersed in an ethanol:DIW solution (1:1 v/v) for 30 min. Then 2.8 ml of 0.1 M Pt and 3.3 ml of 0.1 M Ce precursors dissolved in ethanol:DIW (1:1 v/v) were added drop by drop to the MWCNTs, and the mixture was sonicated for 30 minutes. The resulting ink was transferred onto a quartz crucible and placed in a tubular furnace. The temperature was increased at the rate of 3 °C per minute and the reduction process took place at 300 °C under H_2 atmosphere for 3 hours. The electrocatalyst was then filtrated and washed with abundant DIW. The resulting powders were dried in an oven at 80 °C for 90 min and grinded.

2.2. Physicochemical characterization

SEM-EDS analyses of Pt- CeO_x /MWCNT were performed with a Jeol model JSM 6300 microscope working at 40 kV. Semiquantitative microarea elemental analyses were obtained with an energy dispersive X-ray set-up coupled to the Jeol apparatus. The electrocatalyst was characterized in a Philips X'Pert diffractometer using a Cu K α radiation source ($\lambda_{\text{CuK}\alpha 1} = 1.54060 \text{ \AA}$). Diffractograms were acquired over 10-100 degrees with 0.025 steps and the XRD patterns were identified with the JCPDS data base. The HRTEM studies were carried out in a field emission gun microscope FEI-TITAN 80-300 kV, operated at 300 kV. XPS analyzes were taken in a Perkin-Elmer ESCA/SAM 560, with a base pressure of 1×10^{-9} Torr. The binding energies were calibrated with reference to the Cu $2p_{3/2}$ (932.4 eV) and Cu $3p_{3/2}$ (74.9 eV). To correct any shifts due to electrostatic charges, the C 1s peak (284.6 eV) was taken as reference.

2.3. Electrode preparation and electrochemical setup

The preparation of the catalyst ink has been reported elsewhere [2]. Briefly, the electrocatalyst was mixed by ultrasound to form a catalyst ink of 5 $\text{mg}_{\text{catal}}/\text{mL}$. An aliquot of 10 mL was pipetted onto

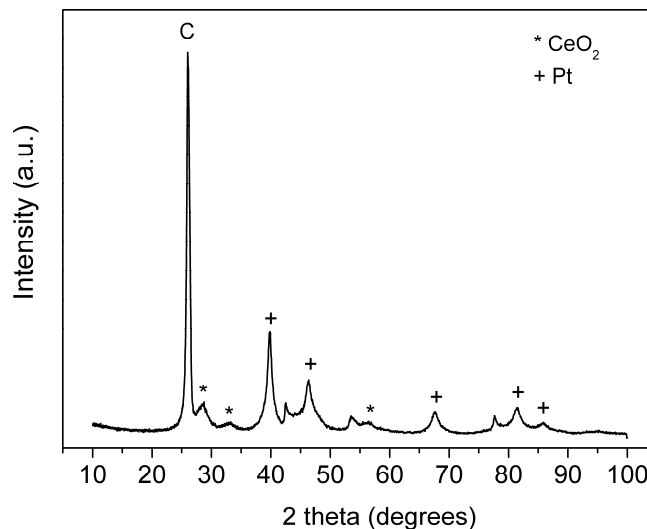


Figure 1. XRD pattern of Pt- CeO_x /MWCNT.

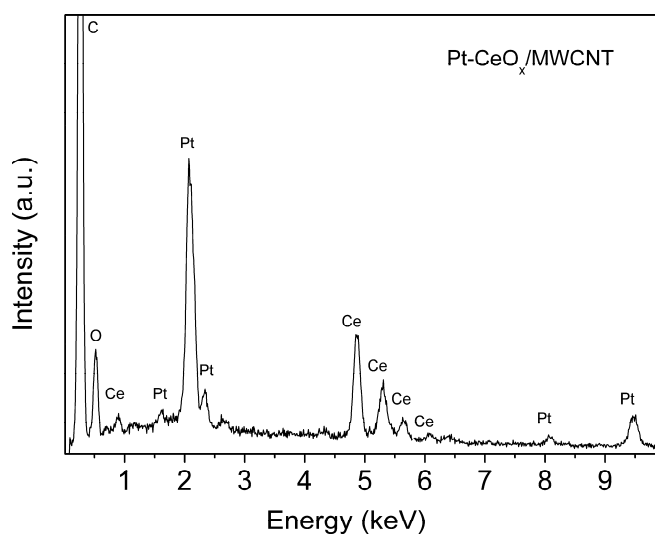
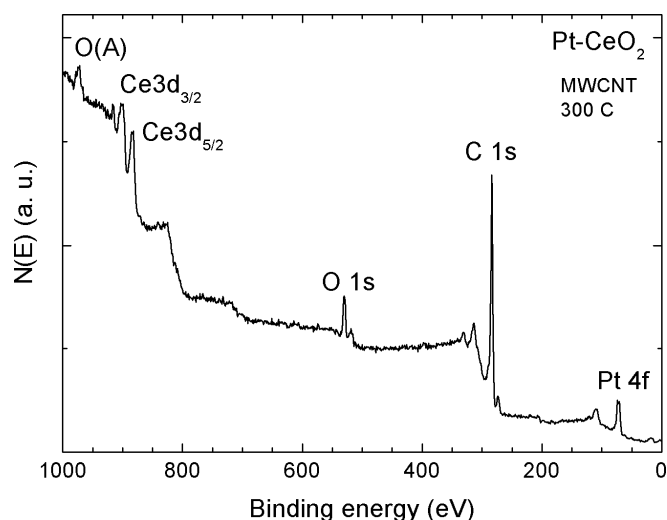
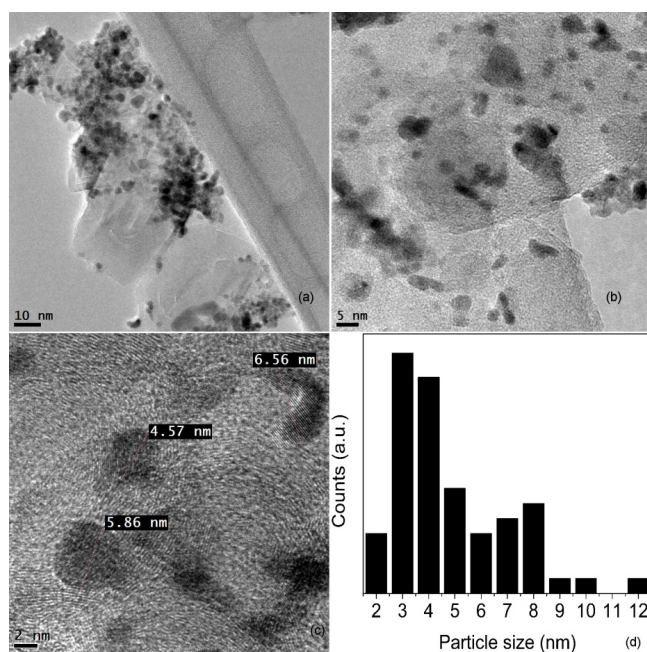
a glassy carbon disc (0.5 cm diam). The working electrodes were characterized using a potentiostat (Voltalab) connected to a RDE set-up (Pine Inst.) at 25 °C. The counter electrode was a platinum mesh while an Ag/AgCl was the reference electrode. Cyclic voltammograms (CV) were obtained at 10 mV/s in N_2 -saturated 0.5 H_2SO_4 . After activation, linear scan voltammetry (LSV) measurements were performed at 10 mV/s in O_2 -saturated 0.5 MH_2SO_4 or 0.5 M H_2SO_4 containing 0.5 M $\text{C}_2\text{H}_5\text{OH}$. All potentials are reported with reference to the standard hydrogen electrode (SHE).

3. RESULTS AND DISCUSSION

Figure 1 shows the XRD pattern of the Pt- CeO_x /MWCNT cathode. The typical diffraction peaks of fcc Pt (1 1 1), (2 0 0), (2 2 0), (3 1 1) and (2 2 2), as well as that of the (0 0 2) graphite plane can be observed. Reflections indexed to CeO_2 (1 1 1) and (3 1 1) planes are clear at $2\theta = 28.4$ and 56.1 . The ceria (2 0 0) peak is merged with the Pt (2 0 0) reflection at 46.6 . The results indicate that there is no influence of CeO_2 in the crystallographic orientations of Pt by shifting any of its diffraction peaks or by the formation of Pt-Ce alloying, and are consistent with the literature [9, 10, 16]. With the use of the Scherrer equation [2], the average particle size d was determined by analyzing the (2 0 0) and (3 1 1) reflections of Pt and Ce, respectively and are given in Table 1. The d value calculated for Pt is nearly 10 nm, a little higher than previous reports for similar electrocatalysts [16]. Meanwhile d is around 1.7 nm for Ce. The broadening of the (3 1 1) CeO_2 peak and its small particle size

Table 1. Physicochemical characteristics of Pt- CeO_x /MWCNT

	EDS (w/o)	d , XRD (nm)	d , TEM (nm)
Pt	7	10	Particles in the 2-12 nm range
Ce	8	1.7	
MWCNT	78	-	-

Figure 2. EDS spectrum of the Pt-CeO_x/MWCNT cathode.Figure 4. Overall XPS spectra of Pt-CeO_x/MWCNT.Figure 3. HRTEM images of the Pt-CeO_x dispersed on commercial MWCNTs. The particle size histogram is included.

calculated from the Scherrer equation are in good agreement with the literature [17].

The chemical composition of Pt-CeO_x/MWCNT was evaluated by EDS. A typical spectrum is presented in Figure 2, in which for a better view of the results, the full scale of C is not shown. The analysis indicates that the mass weight percent (w/o) is around 7 and 8 for Pt and Ce, respectively. Moreover, the mass fraction of MWCNT is 78%, values consistent with our initial theoretical calculations. The results are shown in Table 1.

Figure 3 shows HRTEM images of the Pt-CeO_x/MWCNT electrocatalyst. The pictures in Figures 3(a) and 3(b) show the disper-

sion of the Pt and Ce nanoparticles along the support. The distribution is not as homogeneous as expected, and some agglomerates were formed. As can be seen, the morphology of the commercial nanotubes is highly heterogeneous, with not so well defined nanotube-like forms and the structure shows some agglomerations. The detailed image in Figure 3(c) shows Pt and Ce nanoparticles, with diameters in the 2 - 7 nm range. It was not possible to distinguish Pt from Ce nanoparticles, but the average particle size is of the same order as those obtained from XRD analysis. Figure 3(d) show the particle size histogram of the Pt-CeO_x electrocatalyst.

Figure 4 shows the XPS spectra of Pt-CeO_x/MWCNT. Peaks that correspond to all of the elements in the electrocatalyst can be clearly distinguished.

The detailed spectra of Ce and Pt are depicted in Figure 5. The Ce 3d components are well defined in Figure 5(a). The broad shoulders of Ce_{3/2} and Ce_{5/2} include Ce³⁺ and Ce⁴⁺ signals [18]. In our measurements, the intensities of the peaks corresponding to Ce³⁺ (886.4 and 904.3 eV) are practically the same as those of Ce⁴⁺ (883.2 and 901.5 eV) at both Ce 3d signals. The shape of such spectrum is consistent with that of a material having combined phases of Ce₂O₃ and CeO₂. This conclusion is in good agreement with previous reports [18 and reference therein], where the authors reported Ce³⁺ and Ce⁴⁺ peaks at the Ce_{3/2} and Ce_{5/2} signals of ceria. In the case of a so-called reduced ceria close to CeO₂ the peaks related to Ce⁴⁺ were clearly dominant, while Ce³⁺ peaks were significantly more intense at well-oxidized ceria (Ce₂O₃) [18]. Moreover, the same conclusion can be obtained for the XPS results in reference [15], where the dominant peaks at the Ce_{3/2} and Ce_{5/2} signals were those of Ce³⁺, and the material was labeled as CeO_x. Accordingly, from our XPS analysis we may conclude that the cerium oxide contained in the composite cathode is a mixture of Ce₂O₃ and CeO₂ phases. Thus, the presence of the Ce³⁺ state in the cerium cocatalyst is very important in order to have a material with catalytic activity for the RRO and tolerance to organic molecules, as we will see later in this paper. In opposition, a material with a predominant Ce⁴⁺ state gives as a result a material with high catalytic activity as anode for the direct oxidation of organic molecules [11-14].

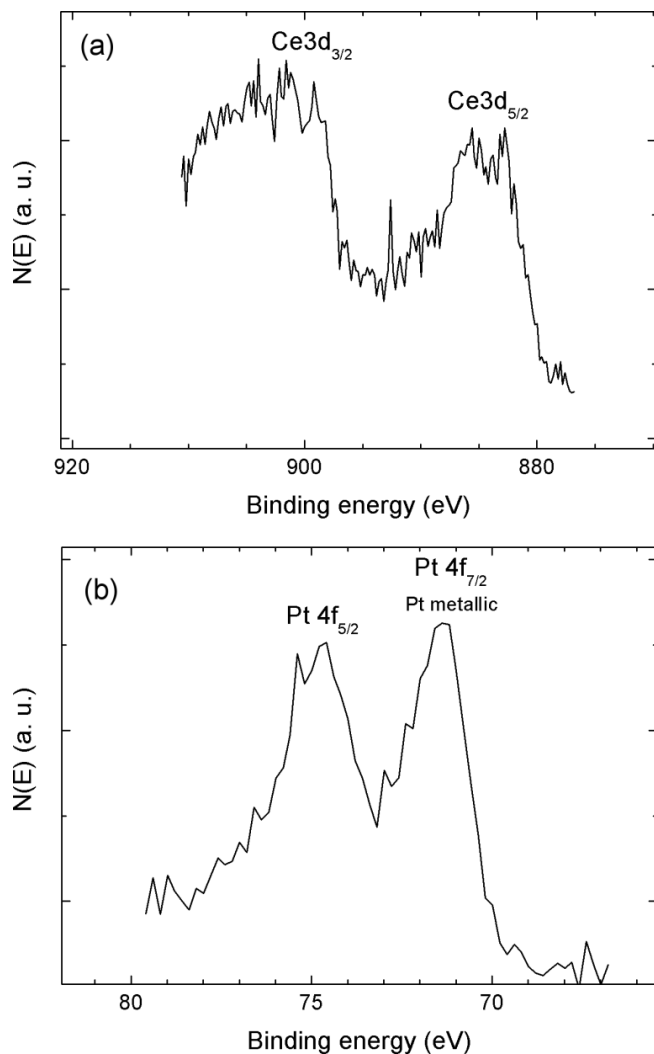


Figure 5. XPS spectra of the Ce 3d (a) and Pt 4f (b) regions for the Pt–CeO_x/MWCNT electrocatalyst.

At the same time, the analysis of the 4f_{7/2} Pt peak at around 71.4 eV in Figure 5(b) confirms the presence of metallic Pt, a result that is in good agreement with previous reports in the literature [15].

Figure 6 shows the ORR polarization curves on the commercial Pt/C cathode at different values of ω (400, 800, 1200 or 1600 rpm). Also, the polarization curve of the ORR in the presence of 0.5 M C₂H₅OH at 1600 rpm is depicted in this Figure (solid line). The well known loss of performance of Pt-alone cathodes is clearly observed in the presence of EtOH. E_{onset}^{ORR} shifts ca. 500 mV from its value without to its value with organic molecule, a poor behavior of Pt/C that has been also observed with other liquid fuels [2,18-20].

Figure 7 shows the ORR curves at Pt-CeO_x/MWCNT. The rotating rates were the same as in Figure 6. The shape of the polarization curves exposes the kinetic, mixed and mass transport limited regions. E_{onset}^{ORR} is around 0.9 V vs SHE, slightly lower than in the case of the Pt/C catalyst in the absence of ethanol in Figure 6 (1.08

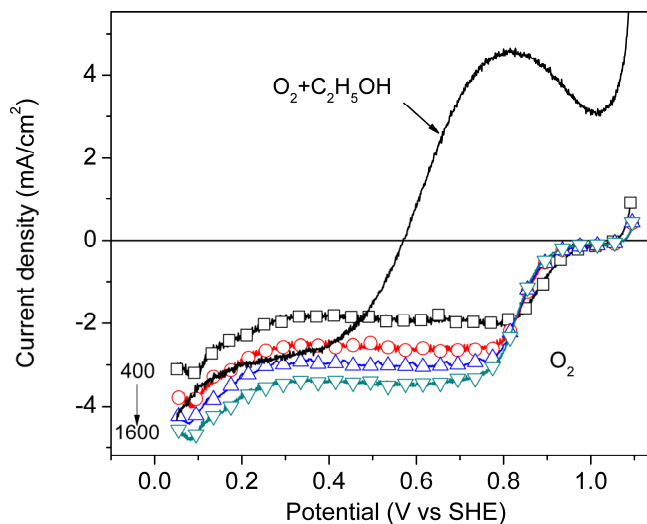


Figure 6. ORR polarization curves at Pt/C. Electrolyte: 0.5 M H₂SO₄. The solid line indicates the polarization curve of the ORR at this catalyst in the presence of 0.5M C₂H₅OH with $\omega=1600$ rpm. Scan rate in both measurements: 10 mV/s.

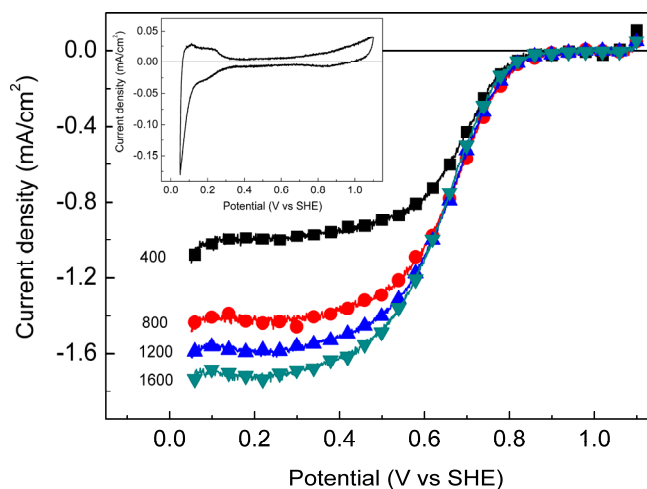


Figure 7. ORR polarization curves at Pt-CeO_x/MWCNT. Electrolyte: 0.5 M H₂SO₄. Inset: CV of Pt-CeO_x/MWCNT in N₂-saturated solution. Scan rate in both measurements: 10 mV/s.

V vs SHE). The inset in Figure 5 shows the CV of the Pt-CeO_x/MWCNT cathode. As expected, the shape is that of a Pt-like electrocatalysts.

Levich-Koutecky lines corresponding to Pt-CeO_x/MWCNT are presented in Figure 8. The lines were plotted from the experimental results in Figure 7 and calculated from the well known Levich equation taking into account literature parameters [2]. The experimental slopes are quite similar to the theoretical slope that corresponds to a 4e⁻ pathway, also shown in the Figure. As a reference, the theoretical slope of a 2 e⁻ mechanism is also presented. These results clearly suggest an overall 4 electron transfer mechanism of the ORR at the Pt-CeO_x/MWCNT cathode.

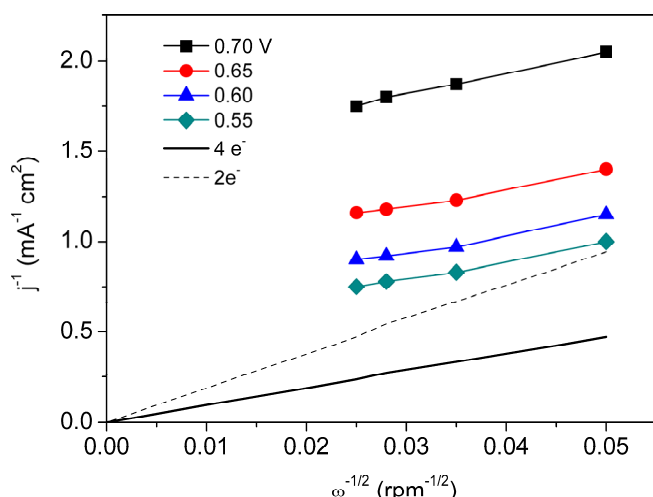


Figure 8. Levich-Koutecky slopes of the ORR at Pt-CeO_x/MWCNT, from experimental results in Figure 5.

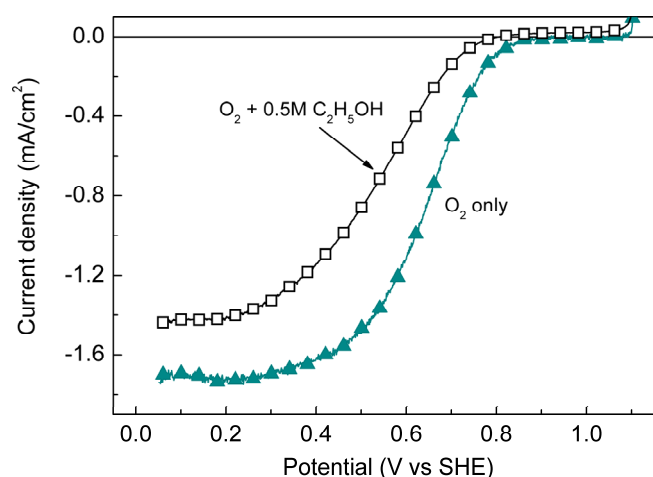


Figure 9. LSVs of the ORR at Pt-CeO_x/MWCNT in the absence and presence of 0.5 M C₂H₅OH in 0.5 M H₂SO₄. Scan rate: 10 mV/s. ω : 1600 rpm.

Figure 9 shows the polarization curves of the ORR at Pt-CeO_x/MWCNT without and with 0.5 M C₂H₅OH. The onset potential shifts by only ca. 80 mV in the presence of ethanol related to the value without alcohol, a significantly smaller change compared to the very important variation at the Pt-alone electrocatalysts in Figure 6 and in previous works [18-20]. Another relevant characteristic of Pt-CeO_x/MWCNT in the ethanol-containing solution is the absence of a peak current density associated to the EOR.

Therefore, the introduction of cerium oxide (a mixture of Ce₂O₃ and CeO₂ phases as determined from XPS measurements) in the structure of the composite cathode clearly enhances the tolerance of Pt-based electrocatalysts, improving its selectivity towards the ORR by acting as oxygen buffer, most probably providing intermediates that may accelerate the reaction of O_{ads} species. The second function of cerium oxide is to supply additional oxygen-containing intermediate groups that may be a source of hydroxide or water

molecules that weaken the adsorption strength of the liquid fuel and/or their intermediates, allowing for the availability of free Pt sites for the ORR. This conclusion can be confirmed by the absence of an oxidation current peak at Pt-CeO_x/MWCNT with ethanol in Figure 9.

4. CONCLUSIONS

This work demonstrates the synthesis of a Pt-CeO_x/MWCNT electrocatalyst by thermal pyrolysis under H₂ atmosphere. The *d* value for Pt in the prepared material is around 10 nm, a larger particle size than those reported in the literature. Attention will be paid to this parameter in our future work. Meanwhile, the *d* value for Ce is around 1.7 nm, in good agreement with the small particle size of ceria-based electrocatalysts previously reported. The XPS analyses of Pt and Ce indicate the presence of metallic Pt and a mixture of Ce₂O₃ and CeO₂ phases. The Pt-CeO_x/MWCNT cathode shows a high catalytic activity for the ORR, with an onset potential near 0.9 V vs SHE. From Levich-Koutecky plot results, we can conclude that the ORR mechanism at this cathode follows a 4 e⁻ pathway. The polarization plots of the ORR in the presence of ethanol clearly demonstrate that Pt-CeO_x/MWCNT is a highly tolerant cathode. Its selectivity and degree of tolerance can be due to the presence of cerium oxide with a valence state of +3.

5. ACKNOWLEDGMENTS

The authors thank the Mexican Council for Science and Technology (CONACYT) for financial support through grant 79870 and the Innovative Networks Program.

REFERENCES

- [1] E. Antolini, T. Lopes and E.R. Gonzalez, *J. Alloys Compd.*, 461, 253 (2008).
- [2] D. Morales-Acosta, L.G. Arriaga, L. Alvarez-Contreras, S. Fraire Luna and F.J. Rodríguez Varela, *Electrochem. Commun.*, 11, 1414 (2009).
- [3] P. Hernández-Fernández, S. Rojas, P. Ocón, A. de Frutos, J.M. Figueroa, P. Terreros, M.A. Peña and J.L.G. Fierro, *J. Power Sources*, 177, 9 (2008).
- [4] O. Savadogo, K. Lee, S. Mitsushima, N. Kamiya and K-I Ota, *J. New Mat. Electrochem. Systems*, 7, 77-83 (2004).
- [5] S. Song, Y. Wang, P. Tsiakaras and P.K. Shen, *Appl. Catal. B*, 78, 381 (2008).
- [6] V. Baglio, A. Stassi, A. Di Blasi, C. D'Urso, V. Antonucci and A.S. Aricò, *Electrochim. Acta*, 53, 1360 (2007).
- [7] P. Nekooi, M. Akbari and M.K. Amini, *Int. J. Hydrogen Energy*, 35, 6392 (2010).
- [8] L. Xiong and A. Manthiram, *Electrochim. Acta*, 49, 4163 (2004).
- [9] H.B. Yua, J.-H. Kim, H.-I. Lee, M.A. Scibioh, J. Lee, J. Han, S.P. Yoon and H.Y. Ha, *J. Power Sources*, 140, 59 (2005).
- [10] X. Wang, W. Xu, X. Zhou, T. Lu, W. Xing, Ch. Liu and J. Liao, *J. Solid State Electrochem.*, 13, 1449 (2009).
- [11] M.A. Scibioh, S.-K. Kim, E.A. Cho, T.-H. Lim, S.-A. Hong, H.Y. Ha, *Appl. Catal. B*, 84, 773 (2008).
- [12] L. Shen, Q.-Z. Jiang, T. Gan, M. Shen, F.J. Rodríguez Varela,

- A.L. Ocampo and Z.-F. Ma, *J. New Mat. Electrochem. Systems*, 13, 205 (2010).
- [13]D.-J. Guo and Z.-H. Jing, *J. Power Sources*, 195, 3802 (2010).
- [14]J. Wang, J. Xi, Y. Bai, Y. Shen, J. Sun, L. Chen, W. Zhu, X. Qiu, *J. Power Sources*, 164, 555 (2007).
- [15]K.H. Lee, K. Kwon, V. Roev, D.Y. Yoo, H. Chang, D. Seung, *J. Power Sources*, 185, 871 (2008).
- [16]R.F.B. De Souza, A.E.A. Flausino, D.C. Rascio, R.T.S. Oliveira, E. Teixeira Neto, M.L. Calegari and M.C. Santos, *Appl. Catal. B*, 91, 516 (2009).
- [17]J.W. Guo, T.S. Zhao, J. Prabhuram, R. Chen and C.W. Wong, *J. Power Sources*, 156, 345 (2006).
- [18]F. Zhang, P. Wang, J. Koberstein, S. Khalid, S.-W. Chan, *Surface Science*, 563, 74 (2004).
- [19]D. Morales-Acosta, D. López de la Fuente, L.G. Arriaga and F. J. Rodríguez Varela, *Int. J. Electrochem. Sci.*, (2011) accepted for publication.
- [20]F.J. Rodríguez Varela, S.E. González Ramírez and R. Dabek Klapco, *J. New Mat. Electrochem. Systems*, 12, 9 (2009).
- [21]F.J. Rodríguez Varela and O. Savadogo, *J. Electrochem. Soc.*, 155, B618 (2008).